Efficient and Sensitive Capacitive Readout of Nanomechanical Resonator Arrays

Patrick A. Truitt,† Jared B. Hertzberg,† C. C. Huang,‡ Kamil L. Ekinci,§ and Keith C. Schwab*,∥

Department of Physics, University of Maryland, College Park, Maryland 20740, Electrical and Computer Engineering Department, Boston University, Boston, Massachusetts 02215, Aerospace and Mechanical Engineering Department, Boston University, Boston, Massachusetts 02215, and Laboratory for Physical Sciences, College Park, Maryland 20740

ABSTRACT

Here we describe *all-electronic* broadband motion detection in radio frequency nanomechanical resonators. Our technique relies upon the measurement of small motional capacitance changes using an LC impedance transformation network. We first demonstrate the technique on a *single* doubly clamped beam resonator with a side gate over a wide range of temperatures from 20 mK to 300 K. We then apply the technique to accomplish multiplexed readout of an *array* of individually addressable resonators, all embedded in a single high-frequency circuit. This technique may find use in a variety of applications ranging from ultrasensitive mass and force sensing to quantum information processing.

Introduction. Nanotechnology derives its power from the unique and useful properties of devices engineered at tiny length scales. Among the most promising of these nanodevices are nanoelectromechanical systems (NEMS).[1] Because of their very small masses, high frequencies, low intrinsic dissipation, and batch fabrication, NEMS have received a great deal of attention in recent years. Potential applications of these devices span a huge range, from ultrasensitive mass[2,3] and force[4,5] sensing to imaging[6] to quantum information processing.[7,8] Development of arrays of NEMS resonators, operating in concert, is especially important for all these emerging sensing, imaging, and data processing technologies.

A central challenge in front of the development of nanotechnology is the detection of signals from nanodevices, i.e., coupling signals efficiently from the microscopic sources at the nanoscale to macroscopic detection circuits. This very challenge has arisen in the field of NEMS as well: detection of microscopic NEMS motion. All of the above-mentioned NEMS applications require robust and sensitive displacement detection if these advanced technologies are to appear outside a laboratory setting. Consequently, much effort has gone into the demonstration and development of nanomechanical

displacement detection schemes based upon a variety of physical phenomena: optical interference,[9,10] piezoresistivity,[11] magnetomotive effect,[12] and motional changes in the electronic properties of low dimensional electronic systems, such as quantum dots,[13] quantum point contacts,[14] carbon nanotubes,[15] and single-electron transistors.[16,17] The most heavily utilized techniques have been the magnetomotive technique and optical interferometry; the latter was used to mechanically detect the atto-newton level force generated by a single electron spin.[5] Some of these techniques are quite sensitive; for instance, displacement sensitivity a factor of 5.8 from the Heisenberg uncertainty limit has recently been achieved at ultralow temperatures by capacitively coupling a single-electron transistor (SET) and an ultrasensitive microwave detection network to a nanomechanical resonator.[17] Unfortunately, most of these techniques are not usable in practical devices due to the extreme conditions necessary for operation such as very large magnetic fields, very low temperatures, or device complexity. Moreover, most are not amenable to the readout of many resonators on a *single* high-frequency channel, i.e., multiplexing.

Here we show that it is indeed possible to realize simple, ultrasensitive, efficient *all-electronic* displacement detection in a radio frequency nanoscale mechanical resonator through capacitive coupling. Furthermore, we demonstrate the application of this capacitive technique to read out the motional response of an array of ∼20 individually addressable

* Corresponding author. E-mail: schwab@ccmr.cornell.edu.
† Department of Physics, University of Maryland.
‡ Electrical and Computer Engineering Department, Boston University.
§ Aerospace and Mechanical Engineering Department, Boston University.
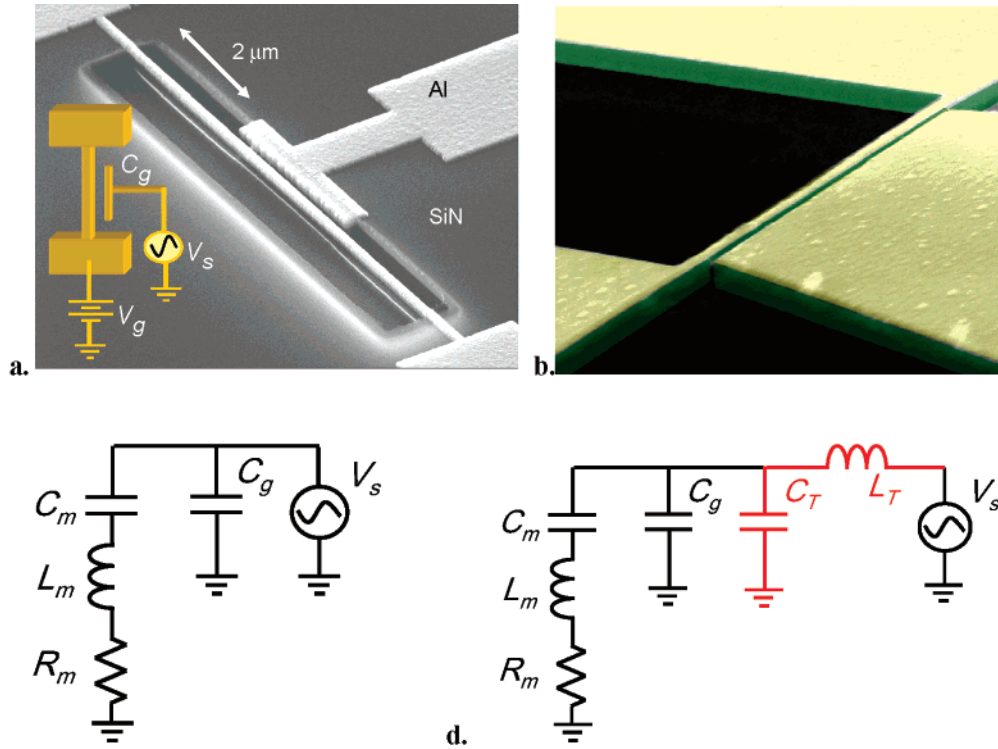∥ Laboratory for Physical Sciences.

Figure 1. (a) Scanning electron microscope (SEM) image of an 11 MHz nanomechanical doubly clamped beam resonator fabricated by surface micromachining. The resonator is 12 μm long, 200 nm wide, and 150 nm thick. It is composed of 100 nm of low-stress silicon nitride, covered with 50 nm of aluminum. It is separated by $d = 180$ nm from an aluminum gate. The inset shows typical device biasing. (b) SEM image of the sample used for room temperature measurements. The doubly clamped beam has dimensions 14 μm $\times$ 200 nm $\times$ 205 nm ($l \times w \times t$) with an 80 nm thick aluminum film on top of a 125 nm thick silicon nitride layer. The gap between the beam and gate is d =130 nm. (c) Equivalent electromechanical circuit of a voltage biased resonator. Currents generated by mechanical motion are modeled by the parallel resonant circuit formed by L_m, C_m, and R_m. (d) Impedance matching LC network. On resonance, the impedances of L_m and C_m cancel, revealing R_m, which is then transformed to a lower value using an LC network formed by L_T and C_T (shown in red). L_T and C_T are located in close proximity to the silicon chip and are formed by chip inductors and an adjustable capacitor which is trimmed such that the LC resonance is coincident with the nanomechanical resonance. In the simplest model, the losses in the LC can be characterized using a parasitic resistance R_T attached in series to L_T (not shown).

resonators, with no apparent degradation in detection sensitivity, all on a single high-frequency circuit. This technological advance is expected to enable a host of NEMS-based applications: very high-frequency (VHF) communication filters, operation of NEMS sensor arrays, ultrasensitive force microscopy, and quantum-limited amplification and readout of quantum information devices.[7]

Readout of a Single Nanomechanical Resonator. One of the simplest and most utilized methods to detect the small motion of a macroscopic object is based on the measurement of the change in capacitance between the object and a fixed electrostatic gate. It is commonly accepted,[18] however, that this method is ineffective for nanoscale mechanical resonators because the motional capacitance change between the resonator and a nearby gate is vanishingly small. A first-pass crude estimate illustrates the challenge very clearly: A $\sim$1 μm long metallic gate separated by $\sim$100 nm from a metallized nanomechanical doubly clamped beam resonator (such as the ones shown in Figure 1a and b) will have a *static* capacitance of $\sim$10^{-17} F, giving an impedance of $|Z_C| = 1/\omega C_g \approx 10^8-10^9$ Ω at a resonant frequency of $\sim$10$-$100 MHz. Nanoscale flexural motion of the beam will change this capacitance by only $\sim$10^{-19} F. In a typical radio frequency measurement with 50 Ω electronics, any *dynamic*

motional signal developing across the resonator-gate structure will be divided down to negligible levels because of the ultrahigh source impedance. In a low frequency measurement with a high input impedance amplifier, the $10^{-12}-10^{-10}$ F of parasitic capacitance, e.g., from cables or contact pads typical between the device and the measurement electronics, will deteriorate the signal and the available bandwidth.

The above line of reasoning is accurate in describing the challenges in the detection of small dynamic capacitance changes. However, the situation changes dramatically when a static voltage V_g is applied between the resonator and the nearby gate. One can show, by using Ohm's law and Newton's second law, that the equivalent impedance network in Figure 1c describes the electromechanical motion of the one-dimensional damped harmonic resonator accurately when the resonator-gate structure is voltage biased. This impedance network comprises the gate capacitance C_g in parallel with a series RLC circuit, where $L_m = d^2m/V_g^2C_g^2$, $C_m = V_g^2C_g^2/\omega_0^2d^2m$, and $R_m = d^2m\,\omega_0/(V_g^2C_g^2Q)$. Here, m is the effective (lumped) resonator mass, d is the equilibrium gap between the gate and the resonator center, and ω_0 and Q are the nanomechanical resonant angular frequency and the quality factor, respectively. We have made the approximation $\partial C_g/\partial x \cong -C_g/d$, assuming that the displacement $x(t)$ of the beam

center is small, $x(t) \ll d$. Given the electromechanical model of the resonator, the equivalent impedance $Z_T(\omega)$ through the gate electrode is given by

$$\frac{1}{Z_T(\omega)} = i\omega C_g + \frac{1}{i\omega L_m - \dfrac{i}{\omega C_m} + R_m} \qquad (1)$$

To gain further insight into the operation of the capacitive technique, let us establish more concrete values for the components in the electromechanical circuit model. Using the parameters for a typical nanomechanical resonator, such as the one shown in Figure 1a (see data in Figure 2b as well: $m \approx 1.2 \times 10^{-15}$ kg, $Q \approx 26500$, $\omega_0/2\pi \approx 11$ MHz, and $C_g/d \approx 0.3$ aF/nm, with $C_g \approx 54$ aF, $d \approx 180$ nm), one finds that $L_m \approx 59$ H, $C_m \approx 3.6$ aF, and $R_m \approx 153$ kΩ for $V_g = 15$ V. This is a rather unusual set of impedances, but nonetheless, they accurately model the electromechanical behavior. This impedance model is well-known in the MEMS community and forms the basis of lower frequency MEMS
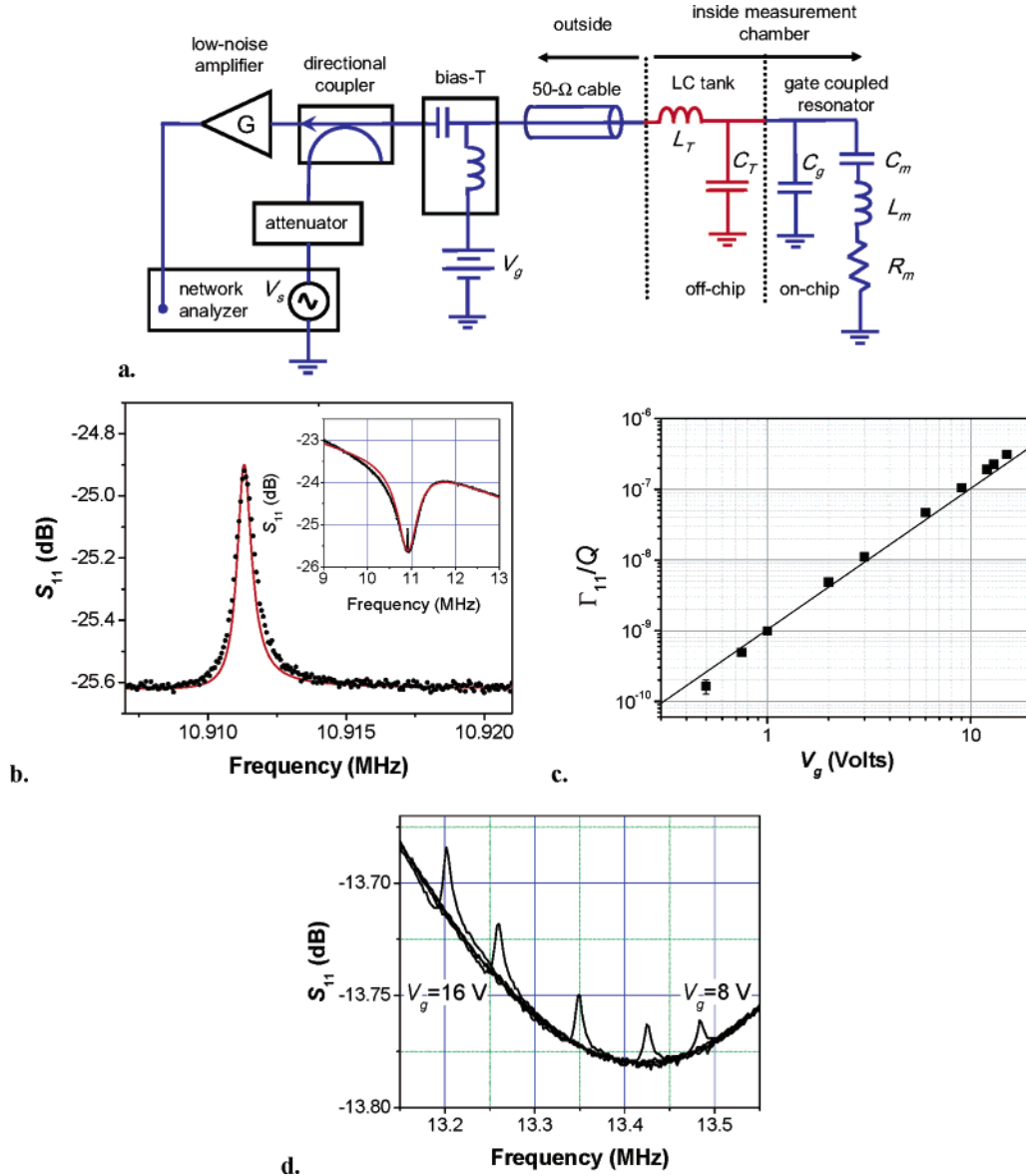

Figure 2. (a) Schematic of the measurement circuit. (b) The measured reflectance data (black points) for device of Figure 1a, taken at 4 K. The inset shows a wider 5 MHz frequency scan, showing the -1.7 dB absorption *dip* due to the losses in the chip inductors ($\sim$600 Ω). The nanomechanical resonance is obvious as the central, narrow $+0.7$ dB *peak*. The line width of the nanomechanical resonance agrees well with magnetomotive measurements. Red curves in both plots are fits using $C_T = 2.2$ pF, $Z_L = 604 + i\,6950\ \Omega$ ($L_T = 94\ \mu$H, $R_T = 600\ \Omega$) along with the resonator impedances $L_m \approx 59$ H, $C_m \approx 3.6$ aF, and $R_m \approx 153$ kΩ at ($V_g = 15$ V). The reflectance change at the nanomechanical resonance is consistent with the electromechanical impedance adding $\sim$300 Ω, placing the circuit further from 50 Ω. (c) The size of the reflected nanomechanical resonance signal vs V_g, demonstrating the expected V_g^2 behavior of R_m. Signal amplitude at each point is normalized by measured Q to account for loading behavior at higher V_g values (see Figure 3b). Solid line is amplitude calculated from physical parameters of part b. (d) Room-temperature measurements. Here the curves show reflection from the circuit at different V_g taken in 2 V steps. The electrical tank components are $C_T = 4.21$ pF, $Z_L = 470 + i\,2800\ \Omega$ ($L_T = 33\ \mu$H, $R_T = 470\ \Omega$). The resonator has $L_m \approx 4.94$ H, $C_m \approx 28.1$ aF, and $R_m \approx 571$ kΩ (at $V_g = 10$ V). Note that to get good fits to room-temperature data, the circuit model may need to incorporate parasitic capacitances.

filters.[19] A key point is that, away from the resonance, the impedance is given by the gate capacitance $|Z_T| \approx 1/\omega C_g$, which is very large. However, on resonance, the impedance drops dramatically to $|Z_T| \approx R_m$.

To couple efficiently into the above-described electromechanical impedance change, an impedance transformation using an LC network, as shown in Figure 1d, can be implemented. If the resonance of the LC network ω_{LC} is degenerate with the nanomechanical resonance, i.e., $\omega_{LC} = \omega_0$, the equivalent on-resonance impedance at the input of the LC network will be given by $Z_{Total}(\omega_0) \approx Z_{LC}^2/R_m + R_T$. Here, $Z_{LC} = \sqrt{L_T/C_T}$ is the characteristic impedance of the LC resonator, and R_T is any additional ohmic impedance that may come from the losses in the inductor (typically important) and the ohmic resistance of the nanomechanical resonator (typically unimportant). In the ideal case where $R_T \rightarrow 0$ and $Z_{Total}(\omega_0) = 50\ \Omega$, all the incoming electrical power would be turned into nanomechanical energy and dissipated in the mechanical resonator, i.e., the resistor R_m. In practice, one minimizes R_T and makes L_T and C_T such that $Z_{Total}(\omega_0)$ approaches 50 Ω. In this case, which is demonstrated below, one couples some of the power into and out of the resonator, but most importantly, obtains enough contrast in a frequency sweep to resolve the electromechanical resonance line shape. As shown below, this provides a powerful approach to detect the nanomechanical resonant motion.

We have demonstrated this readout technique using two similar nanomechanical resonator designs. Parts a and b of Figure 1 show the devices used at low temperature (20 mK to 4 K) and room temperature, respectively. The metallized resonator shown in Figure 1a is surface micromachined out of silicon nitride by a series of electron-beam lithography steps combined with a selective plasma etching process. An aluminum gate is also fabricated nearby, with a gap of d = 180 nm. The dimensions of the doubly clamped beam are 12 μm × 200 nm × 150 nm ($l \times w \times t$). The resonance parameters of the device are easily identifiable using a magnetomotive readout; we find that the fundamental in-plane flexural resonance frequency is at $\omega_0/2\pi \approx 11.2$ MHz with $Q \approx 26500$ at 4.2 K. The device shown in Figure 1b has dimensions of 14 μm × 200 nm × 205 nm ($l \times w \times t$) with an 80 nm thick aluminum film on top of a 125 nm thick silicon nitride layer. The gap between the beam and the gate is $d = 130$ nm. This resonator has $\omega_0/2\pi \approx 13.5$ MHz and $Q \approx 1800$ at room temperature, as confirmed by optical measurements.

Next, we determine the impedance values for the matching network for the devices in Figure 1a and b. For the device in Figure 1a operated at low temperature, to transform R_m ~153 kΩ (at $V_g = 15$ V) to a value close to 50 Ω, we use a LC network[20] formed by a 94 μH inductor together with a 2.2 pF capacitor formed by an adjustable capacitor. This LC network is carefully tuned to resonate at the nanomechanical resonance[21] and gives $Z_{LC} = 6.6$ kΩ. Neglecting resistance R_T in the tank circuit components, this yields an impedance on resonance of $Z_{Total}(\omega_0) = 285$ Ω. For the device in Figure 1b operated at room temperature, $L_m \approx 4.94$ H, $C_m \approx 28.1$ aF, and $R_m \approx 571$ kΩ for a bias voltage $V_g = 10$ V. Here,

we use an LC network formed by a 33 μH inductor and a 4.21 pF capacitor, resulting in $Z_{LC} = 2.8$ kΩ.

We use a radio frequency reflectometry circuit with a 50 Ω characteristic impedance to measure the impedance of the combined nanomechanical resonator−LC network, as shown in Figure 2a. We stimulate the circuit through a directional coupler and provide a dc voltage bias V_g through a bias-tee. The amplitude V_R of the reflected wave is a measure of the deviations of $Z_{Total}(\omega)$ from 50 Ω: $\Gamma(\omega) = V_R/V_I = (Z_{Total}(\omega) - 50\ \Omega)/(Z_{Total}(\omega) + 50\ \Omega)$, where V_I is the amplitude of the incident wave. Figure 2b (main figure) shows the measured reflectance, $S_{11}(\omega) = 20 \cdot \log_{10}|\Gamma(\omega)|$ (in dB), obtained from the device in Figure 1a. The broader sweep (inset), showing the overall circuit response, is valuable in revealing how this technique works. Away from the LC resonance, $Z_{Total}(\omega)$ is reactive, reflecting most of the incoming power. Around the LC resonance, a dip starts to emerge due to the power absorbed in the LC network, reducing the reflected portion of the power. Note that this power is absorbed in R_T, not the resonator itself, because the electromechanical impedance of the nanomechanical resonator is still very large and reactive. In the vicinity of the nanomechanical resonance, the resonator impedance becomes real and adds to R_T, taking the circuit further away from 50 Ω. This is the sharp central peak with $\Delta S_{11}(\omega) \approx 0.7$ dB change in reflectance observed in Figure 2b. Figure 2c shows the size of the reflected signal due to the nanomechanical resonance as a function of V_g. All the presented data is consistent with the simple electromechanical model of Figure 1b, as demonstrated by the accuracy of the fits (solid lines). The corresponding measurements on the device of Figure 1b performed at room temperature are shown in Figure 2d. The reflection signal $S_{11}(\omega)$ is shown at different values of V_g. At room temperature, the lower resonator Q value makes the signal sizes significantly smaller (~0.05 dB); nevertheless, a sufficient contrast in the reflection signal is available. At room temperature, the circuit model must be modified to include additional on-chip capacitance due to the conductivity of the substrate.

The displacement sensitivity $\sqrt{S_X}$ of this technique is limited by the total voltage noise $\sqrt{S_V}$ appearing at the input of the amplifier due to amplifier voltage and current noise, and the quality of the impedance match between the nanomechanical source and amplifier. If the impedance matching network is lossless, $R_T = 0\ \Omega$, then we find that $\sqrt{S_X} = (C_T/C_g)\ (d/V_g)\ \sqrt{S_V}$. In our experiments, the radio frequency amplifier (Miteq model AU-1464) has a measured noise temperature of ~70 K, which would give an ideal sensitivity of $\sqrt{S_X} = 2.1 \times 10^{-13}$ m/$\sqrt{\text{Hz}}$, which is on par with optical interferometry and magnetomotive detection. The resistive losses in the inductor ($R_T = 600\ \Omega$), as well as imperfect transformation of the mechanical resistance to 50 Ω, leads to a degradation of the position sensitivity. We estimate that, for our realization, $\sqrt{S_X} = 4.1 \times 10^{-12}$ m/$\sqrt{\text{Hz}}$ when $V_g = 15$ V. Working with inductors with lower resistive losses would significantly help our circuit approach the ideal sensitivity.

The nanomechanical resonator, in essence, is an energy storage device, where a small amount of the input power is
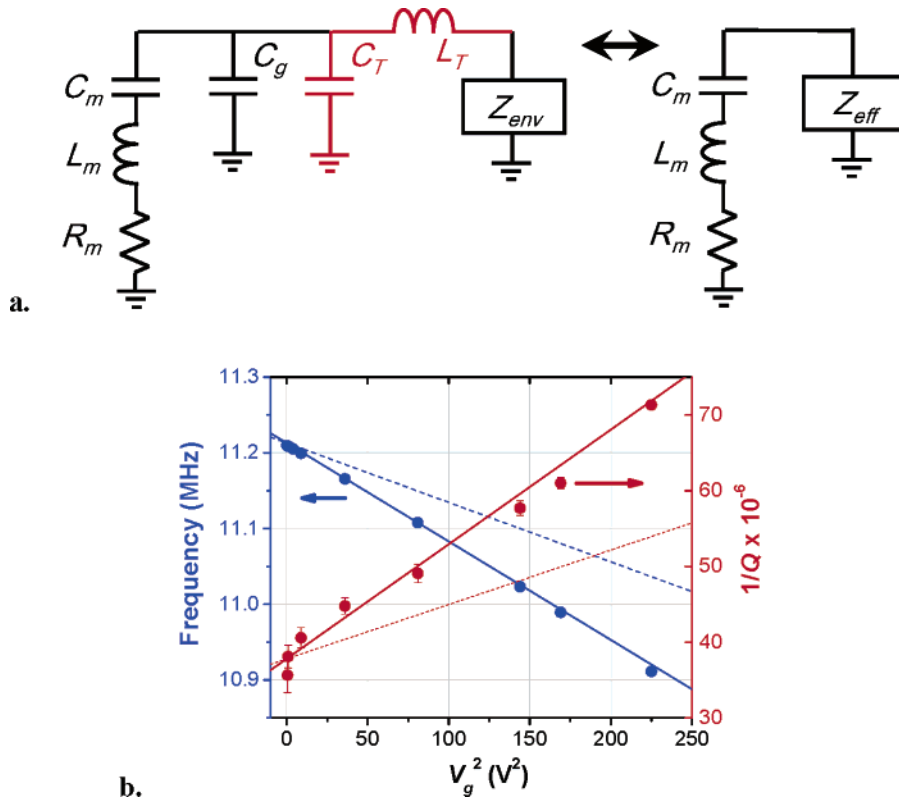
Figure 3. (a) Circuit model showing the effect of the embedding impedances on the electromechanical resonance measurements. Here, the resonator is coupled to the LC impedance matching network and the rest of the measurement circuit indicated by Z_{env}. In our measurements, Z_{env} is 50 Ω; however, it can be engineered to have a different value. The effective impedance Z_{eff} will load the series RLC circuit L_m, C_m, R_m, and modify the measured resonance parameters. {Im}{Z_{eff}} will shift the resonator frequency (a small effect in our circuit) and {Re}-{Z_{eff}} will add to the resistive impedance R_m, lowering the quality factor. (a) Frequency shift and damping versus V_g^2. Frequency shift is primarily due to the electrostatic spring constant $k_e = -(\partial^2 C_g/\partial x^2)(V_g^2/2)$, while the additional damping is due to the dissipation in the loaded circuit. In our realization, the external dissipation is dominated by the resistive impedance of the tank inductor ($R_T \approx 600$ Ω). In the plot appear both theoretical predictions (dashed lines) based on the same parameters as the fits of Figure 2b, as well as best-fit lines (solid lines), demonstrating the expected dependence on V_g^2.

dissipated in every cycle due to the mechanical losses intrinsic to the resonator. An important characteristic of an efficient readout technique is that there is no additional electrical power dissipation and subsequent temperature rise upon the resonator. In the capacitive scheme, the amount of power dissipated in the nanomechanical resonator and its matching network is given by $P = \frac{1}{2} V_s^2/Z_0 (1 - |\Gamma|^2) \approx 5 \times 10^{-12}$ W for the measurements shown in Figure 2, where V_s is the source amplitude and $Z_0 = 50$ Ω is the cable impedance. Because both the matched load impedance, Z_{LC}^2/R_m, and the tank losses, R_T, are comparable in these experiments, the power is deposited on both resistors with roughly equal magnitude. Given that the ohmic resistance of a typical metallized nanomechanical resonator is ~10 Ω, much smaller than R_m, the power dissipated on the device is essentially dominated by the intrinsic mechanical losses. This is much more efficient than the piezoresistive technique, for instance, which dissipates 10^{-6} W for similar detection sensitivity.[22] These heating considerations become especially important at ultralow temperatures given the tiny resonator heat capacity.

The external measurement circuit is expected to affect the nanomechanical resonance, as illustrated in Figure 3a. The finite embedding impedances from the measurement circuit load the electromechanical elements L_m, C_m, and R_m and

modify the intrinsic dissipation and the resonance frequency. This is similar to the case of magnetomotive detection and has been discussed in detail.[23] Figure 3b shows the effects of the coupling voltage V_g between the resonator and the external circuit upon the measured nanomechanical Q factor and resonance frequency; both follow the expected V_g^2 dependence (solid line), albeit with a minor discrepancy in the prefactor (dashed line). We note that, in our realization, the dominant source of additional dissipation is the resistive impedance of the chip inductors; this could be reduced by higher quality inductors.

Readout of Nanomechanical Resonator Arrays. Perhaps the most important feature of this measurement technique is that it allows many nanomechanical resonators with closely separated resonance frequencies to be detected on a single radio frequency readout circuit without any sensitivity loss. Because for each nanomechanical resonator, the impedance away from the resonance is much greater than that on resonance (for instance, a factor of ~10^3 in our demonstration at ~10 MHz), multiple resonators with their gates connected in parallel do not load the circuit except in the vicinity of their individual resonances. This attractive array readout scheme becomes readily implementable on an array of nanomechanical resonators with identical dimensions fabricated on the same chip. Because of their extreme sensitivity

to minor mass fluctuations and high Q factors, such resonators always possess well-separated resonances: $|\omega_j - \omega_{j+1}| \gg \omega_j/Q_j$, where ω_j and Q_j are the resonance frequency and the quality factor of resonators with close-by resonance frequencies, respectively. In addition, each resonator or group of resonators may be voltage biased independently, allowing for selective readout, i.e. addressability, of each resonator.

In the most general array implementation, resonators are grouped into banks; each bank can be biased at a separate dc potential. The impedance of the "kth" resonator bank, biased by dc voltage V_k, is then given by

$$\frac{1}{Z_k(\omega,V_k)} = \sum_j i\omega C_g^j + \frac{1}{i\omega L_m^j - \dfrac{i}{\omega C_m^j} + R_m^j} \qquad (2)$$

where the index j identifies each resonator in the kth bank, and the dependence of L_m^j, C_m^j, and R_m^j on V_k is the same as above. With each bank connected together at the gates, the total array impedance will be

$$\frac{1}{Z_{\mathrm{array}}(\omega)} = \sum_k \frac{1}{Z_k(\omega,V_k)} \qquad (3)$$

To demonstrate this capability, we have fabricated an array formed by two banks of 10 nanomechanical resonators, giving 20 nearly identical resonators in total, shown in Figure 4a and b. The design and dimensions of each resonator in the array is very similar to those of the one described above (see Figures 1 and 2). The gates of all the resonators are connected together; the LC impedance-matching network is attached to the common gate electrode. The resonators themselves within each bank are connected together and can be biased as a group (see Figure 4b). Figure 4c shows two curves (red and blue), each showing the reflected signal when biasing one of the resonator banks. The data agrees well with our electromechanical impedance model of the circuit. We observe no substantial signal loss in comparison with the readout of a single resonator and expect to be able to read out $\sim10^3$ resonators without any loss of sensitivity.

Given minimal signal degradation, the capacity of the multiplexed readout channel in Figure 4 is determined by the LC tank bandwidth and the average individual resonator line width. The latter arises from the losses in the resonator and is ~10 kHz. The LC tank bandwidth determined by R_T is ~1 MHz. This puts an upper limit of ~100 on the number of resonators that can be multiplexed, assuming that the tank circuit resonance is not tunable. In a future application, where frequency shift detection is employed for mass or force sensing, part of the channel bandwidth must be spared for the frequency shifts. Typical to nanomechanical sensors, however, the magnitude of the mass or force that is to be sensed is miniscule, corresponding to very small frequency shifts. A single molecule sensor, for instance, is expected to display a $\sim10-100$ Hz frequency shift when it registers a typical molecule.[24]

Conclusions and Outlook. The capacitive displacement detection technique enabled by the LC impedance matching
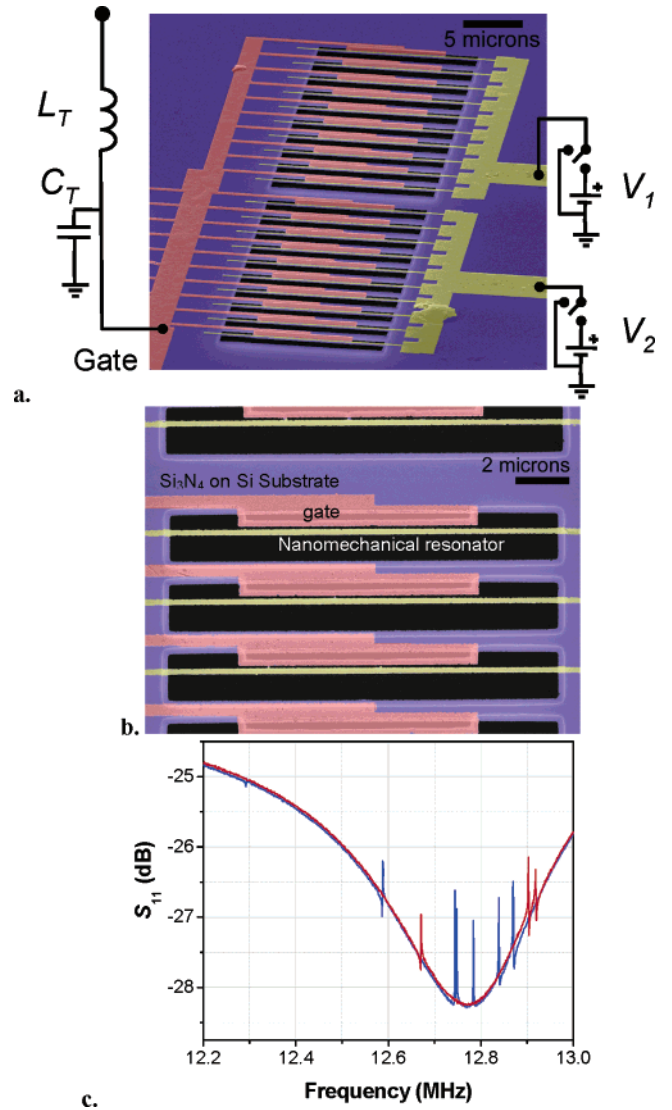

a.

b.

c.

Figure 4. (a) Colorized SEM image of an array of 20 $\sim$12 MHz nanomechanical resonators. Here all the gate leads (marked Gate) are connected; the array is separated into two banks of resonators which can be selectively voltage biased at V_1 and V_2. (b) A close-up image of several beams in the array with nearby gates. The gap between each gate and the accompanying resonator is $\sim$90 nm. The metallized portions of the beams are shown as yellow, the gates red, silicon nitride blue, and the lower silicon layer exposed by the etch as dark gray. (c) Successful readout and addressing of an array of resonators through capacitive coupling. The reflection measurement at this frequency range reveals seven resonators in bank 1 biased at $V_1 = 3$ V (blue curve), and three resonators in bank 2 biased at $V_2 = 3$ V (black curve). Note the large change of $\sim$1 dB in reflectance at various resonances. Modest magnetic field of 0.69 T is used to tune the LC network.[21] Data agrees with our impedance model given in eq 3 (fit not shown).

network appears to be useful for nanomechanical resonators operated under a wide range of environmental conditions (temperature, magnetic field, etc.). Using typical parameters for nanomechanical devices and available components, e.g., chip inductors, we expect operation to be possible from 1 to over 100 MHz. In addition, because the parasitic on-chip capacitance is usually $\sim$0.1 pF, which can be less than the necessary tank capacitance, the nanomechanical resonator arrays demonstrated here do not need to be located in
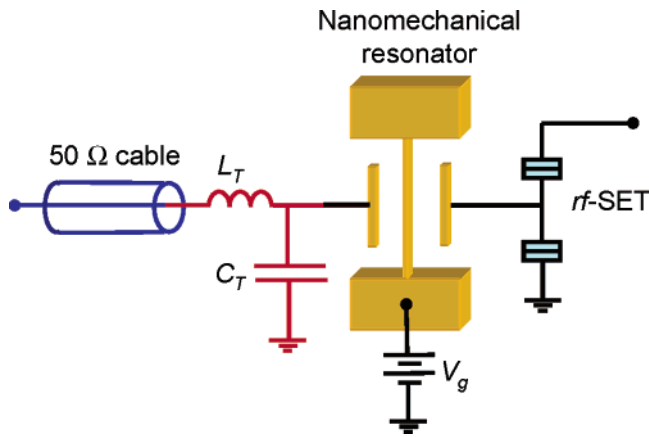
Figure 5. Schematic of proposed quantum-limited narrow band amplifier, which couples signals from low impedance sources, such as cables, to an SET. The signals from the 50 Ω cable are efficiently matched to the nanomechanical resonator using the LC circuit demonstrated in this work. The resulting motion of the mechanical resonator is then detected with the single electron transistor (rf-SET), which has been shown to detect motion very close to the quantum mechanical limit.

microscopic proximity; they could be located millimeters apart, allowing the readout of resonators located on different chips through the same high-frequency circuit. This could facilitate the readout of arrays of chemically or biologically functionalized resonators that have been fabricated using different and incompatible chemistry or processing.

We expect this technique to find utility in a variety of ultralow temperature applications as well. Examples include providing simple and sensitive readout for scanning force microscopy, especially for magnetic resonance force microscopy.[5] We expect to demonstrate a mechanical detection noise temperature of $T_N = 6$ K by implementing an ultralow noise PHEMT amplifier,[25] and by properly impedance matching to this amplifier, $T_N < 1$ K appears possible.

The transformation of the nanomechanical resonator impedance to a low impedance comparable to macroscopic cables can be combined with the recent demonstration of near-optimal coupling of a single-electron transistor (SET) to a nanomechanical resonator;[17] see Figure 5. An SET is a charge amplifier that has been shown to be nearly quantum limited[26] and capable of continuous detection of nanomechanical motion to within 3.9 times the Heisenberg uncertainty principle limit. The LC and the nanomechanical resonator together form an impedance network, which allows a 50 Ω source to be efficiently coupled to an SET, creating a nearly quantum-limited, narrow-band, radio frequency amplifier. This two-step impedance matching (LC + nanomechanics) can solve the difficult problem of coupling an SET to macroscopic circuits and cables. However, this is accomplished over a very narrow band in frequency (determined by the nanomechanical resonator bandwidth), which may be useful for isolation of the SET from unwanted out-of-band noise.

Finally, these techniques are now being implemented into quantum information devices, where shifts in the nanomechanical resonant frequency are expected to provide a quantum nondemolition readout of a capacitively coupled, solid-state charge qubit.[7] By integrating the very compact mechanical resonators with the qubits by surface micromachining, this technique can provide readout of many qubits on a single detection circuit, providing detection at the charge degeneracy point, where the quantum states differ by only a subtle phase factor and the qubits have been shown to be most resistant to decoherence.[27]

References

(1) Roukes, M. L. *Sci. Am.* **2001**, *285,* 48.
(2) Ekinci, K. L.; Huang, X. M. H.; Roukes, M. L. *Appl. Phys. Lett.* **2004**, *84*, 4469.
(3) Ilic, B.; Yang, Y.; Craighead, H. G. *Appl. Phys. Lett.* **2004**, *85*, 2604.
(4) Sidles, J. A.; Garbini, J. L.; Bruland, K. J.; Rugar, D.; Zuger, O.; Hoen, S.; Yannoni, C. S. *Rev. Mod. Phys.* **1995**, *67*, 249.
(5) Rugar, D.; Budakian, R.; Mamin, H. J.; Chui, B. W. *Nature* **2004**, *430*, 329.
(6) Minne, S. C.; Adams, J. D.; Yaralioglu, G.; Manalis, S. R.; Atalar, A.; Quate, C. F. *Appl. Phys. Lett.* **1998**, *73*, 1742.
(7) Irish, E. K.; Schwab, K. C. *Phys. Rev. B* **2003**, *68*, 155311.
(8) Cleland, A. N.; Geller, M. R. *Phys. Rev. Lett.* **2004**, *93*, 070501.
(9) Carr, D. W.; Sekaric, L.; Craighead, H. G. *J. Vac. Sci. Technol.,* B **1998**, *16*, 3821.
(10) Kouh, T.; Karabacak, D.; Kim, D. H.; Ekinci, K. L. *Appl. Phys. Lett.* **2005**, *86*, 013106.
(11) Harley, J. A.; Kenny, T. W. *Appl. Phys. Lett.* **1999**, *75*, 289.
(12) Yurke, B.; Greywall, D. S.; Pargellis, A. N.; Busch, P. A. *Phys. Rev. A* **1995**, *51*, 4211.
(13) Kirschbaum, J.; Hohberger, E. M.; Blick, R. H.; Wegscheider, W.; Bichler, M. *Appl. Phys. Lett.* **2002**, *81*, 280.
(14) Cleland, A. N.; Aldridge, J. S.; Driscoll, D. C.; Gossard, A. C. *Appl. Phys. Lett.* **2002**, *81*, 1699.
(15) Sazonova, V.; Yaish, Y.; Ustunel, H.; Roundy, D.; Arias, T. A.; McEuen, P. L. *Nature* **2004**, *431*, 284.
(16) Knobel, R. G.; Cleland, A. N. *Nature* **2003**, *424*, 291.
(17) LaHaye, M. D.; Buu, O.; Camarota, B.; Schwab, K. C. *Science* **2004**, *304*, 74.
(18) Ekinci, K. L.; Roukes, M. L.; *Rev. Sci. Instrum.* **2005**, *76*, 061101.
(19) Lin, L.; Nguyen, C. T.-C.; Howe, R. T.; Pisano, A. P. Microelectromechanical filters for signal processing. Technical Digest, IEEE Microelectromechanical Systems Workshop, Travemunde, Germany, Feb. 4−7, 1992; pp 226−231.
(20) Two 47 μH chip inductors are used in series. The inductors are surface mount inductors with powdered iron core, model IMC-1210, 46 μH at $B = 0$, obtained from Vishay Dale. The capacitor is a surface-mount screw-type variable capacitor, trimmed by hand.
(21) For the optimum operation of capacitively coupled resonators, the LC matching network needs to be finely tuned to the nanomechanical resonance. After attachment of the desired inductor and capacitor, the capacitor is adjusted by hand to match the LC resonance to the nanomechanical resonance. If further fine tuning of the LC network is needed at low temperatures, this is accomplished *in situ* within the measurement apparatus using static magnetic fields. We have found that ω_{LC} can be tuned by tuning the inductance of the powdered-iron core chip inductors using an external magnetic field. If no magnetic field is available, a varactor capacitor could possibly be used in place of the hand-trimmable capacitor for in situ adjustment of the LC resonance.
(22) Bargatin, I.; Myers, E. B.; Arlett, J.; Gudlewski, B.; Roukes, M. L. *Appl. Phys. Lett.* **2005**, *86*, 133109.
(23) Cleland, A. N.; Roukes, M. L. *Sens. Actuators* **1999**, *72*, 256.
(24) Yang, Y. T.; Callegari, C.; Feng, X. L.; Ekinci, K. L.; Roukes, M. L. *Nano Lett.* **2006**, *6*, 583.
(25) Oukhanski, N.; Grajcar, M.; Il'ichev, E.; Meyer, H.-G. *Rev. Sci. Instrum.* **2003**, *74*, 1145.
(26) Naik, A.; Buu, O.; LaHaye, M. D.; Blencowe, M. P.; Armour, A. D.; Clerk, A. A.; Schwab, K. C. *Nature* **2006**, *443*, 193.
(27) Wallraff, A.; Schuster, D. I.; Blais, A.; Frunzio, L.; Majer, J.; Devoret, M. H.; Girvin, S. M.; Schoelkopf, R. J. *Phys. Rev. Lett.* **2005**, *95*, 060501.

NL062278G